J Biol Inorg Chem (2007) 12:535–542
DOI 10.1007/s00775-007-0205-2

ORIGINAL PAPER

N-terminal iron-mediated self-cleavage of human frataxin: regulation of iron binding and complex formation with target proteins

Taejin Yoon · Eric Dizin · J. A. Cowan

Received: 1 August 2006 / Accepted: 5 January 2007 / Published online: 7 February 2007

Abstract Frataxin is an iron-binding mitochondrial matrix protein that has been shown to mediate iron delivery during iron–sulfur cluster and heme biosynthesis. Mitochondrial processing peptidase (MPP) yields a form of human frataxin corresponding to residues 56–210. However, structural and functional studies have focused on a core structure that results from an ill-defined cleavage event at the N-terminus. Herein we show that the N-terminus of MPP-processed frataxin shows a unique high-affinity iron site and that this iron center appears to mediate a self-cleavage reaction. Moreover, the N-terminus appears to block previously defined iron-binding sites located on the carboxylate-rich surface defined by the helix (α1) and the β-sheet (β1), most likely through electrostatic contact with the carboxylate-rich surface on the core protein, as well as inhibiting iron-promoted binding of the iron–sulfur cluster assembly scaffold partner protein, ISU. The physiological significance of iron-mediated release of the N-terminal residues from this anionic surface is discussed.

Keywords Frataxin · Friedreich's ataxia · Self-cleavage · Iron binding · ISU

T. Yoon · E. Dizin · J. A. Cowan (✉)
Evans Laboratory of Chemistry,
Ohio State University,
100 West 18th Avenue,
Columbus, OH 43210, USA
e-mail: cowan@chemistry.ohio-state.edu

Introduction

Friedreich's ataxia (FRDA) is an autosomal recessive neurodegenerative disease that has been related both to the mitochondrial protein, frataxin, and to mitochondrial iron levels [1–5]. In most patients, expansion of the repeated GAA trinucleotide in the first intron of the gene (encoding frataxin) interferes with transcription [6, 7], and thus the levels of messenger RNA and frataxin protein are severely reduced. Concurrently, the level of mitochondrial iron was observed to be significantly higher in fibroblasts from FRDA patients than in fibroblasts from a control population [8]. The body of published work suggests a strong connection between frataxin and mitochondrial iron metabolism.

Recently, we demonstrated human frataxin to be a viable iron-delivery vehicle for target proteins implicated in both mitochondrial Fe–S cluster (ISU) [9] and heme (ferrochelatase) [10] biosynthesis. Iron delivery to aconitase has also been noted [11]. The iron-delivery properties of human frataxin that we observed are consistent with observations made in studies of the yeast homologue [12–16]. Following mitochondrial import in human cells, the targeting sequence (residues 1–55) is removed in a two-step process by a mitochondrial processing peptidase (MPP) located in the mitochondrial matrix [17]. It is the ''mature'' protein that is the desirable form to study; however, several groups [9, 17, 18] have reported the unexpected cleavage of the N-terminus of the ''mature'' human frataxin to form a truncated product. Such cleavage has been suggested to occur by natural degradation during purification [18] or by an unknown protease [17]. Consequently the available structural information on human frataxin is focused on the core residues defined

by this truncated protein. It is significant that these core residues are conserved across various species. Elsewhere in this paper we will refer to the expressed protein (His-tag and residues 46–210, including the additional N-terminal residues 46–77) as ''full-length'' frataxin, and the self-cleavage product (residues 78–210) as the ''truncated'' form. Unless otherwise stated, both forms of frataxin are generally isolated and used in the metal-free apo form, with metal ions subsequently added as required for specific studies.

The core structure [18, 19] of human frataxin consists of a compact $\alpha\beta$ sandwich with an anionic surface patch that is solvent-exposed (Fig. 1). These negatively charged residues are conserved across various species and are putative iron-binding residues [9]. Recently, several groups have characterized the iron-binding sites of bacterial, yeast and human frataxin [20, 21]. As predicted [9, 10, 21], the iron-binding sites appear to lie mainly on the anionic surface defined by the α1-helix and the β1-sheet.

Clearly frataxin is an important regulator of mitochondrial iron chemistry that merits additional investigation of its functional role, both in mitochondrial iron metabolism and as an iron chaperone. A clear understanding of the overall structure of frataxin and its iron-binding characteristics (including the locations, binding affinity and oxidation state of the bound ion) is critical to evaluating the overall functional chemistry of frataxin in the mitochondrion. In this paper we explore the chemistry underlying the self-cleavage reaction of the MPP-processed frataxin, and possible physiological roles for the N-terminal domain (residues 56–77) in mediating mitochondrial iron metabolism. The N-terminal domain appears to make electrostatic contact with the carboxylate-rich surface on the core protein, blocking binding of previously characterized iron-binding sites on the truncated protein, as well as iron-promoted binding of physiological partners.

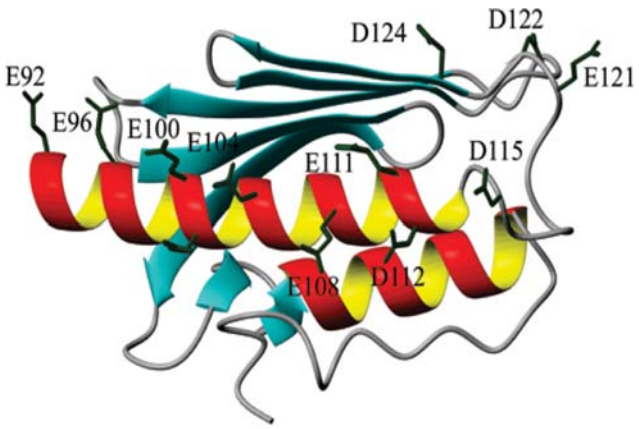

Fig. 1 Ribbon representation of *Hs* frataxin secondary structure (Protein Data Bank ID 1EKG) showing the surface carboxylates that are putative binding sites for iron ions

Materials and methods

General chemicals and procedures

Nitrilotriacetic acid (NTA) resin and DE-52 ion-exchange resin were purchased from QIAGEN (Valencia, CA, USA) and Whatman (Aston, PA, USA), respectively. Homogenous-20 precast polyacrylamide gels, G-25 and Superose-12 resins were purchased from Pharmacia (Bridgewater, NJ, USA). Ethylenediaminetetraacetic acid (EDTA) and 7-diethylamino-3-(4′-maleimidylphenyl)-4-methylcoumarin were purchased from Acros Organics (Morris Plains, NJ, USA) and Molecular Probes, respectively. Buffer solutions were prepared from deionized water produced by a NANOpure Diamond system (Barnstead, IO, USA). Metal salts were prepared under anaerobic condition using argon-purged buffers and were used immediately following preparation. Solutions of ferric ion were prepared by solubilizing $FeCl_3$ in aqueous solution at pH 3, with subsequent immediate addition of a small aliquot to the sample of interest buffered at pH 7.5, or the solution of ferric ion was prepared by use of the ferrous salt, $FeSO_4{\cdot}7H_2O$, and quantitatively oxidized by exposure to air with subsequent argon purge if required.

Protein expression and purification

The procedures have been described previously [9]. In brief, buffer solutions were prepared from NANOpure water, unless otherwise stated. To prevent natural cleavage, the buffer containing His-tagged protein [pET28b(+)-Ftx], described previously [9], was exchanged with 50 mM tris(hydroxymethyl)aminomethane (Tris)–HCl, pH 7.5, 50 mM NaCl and 5 mM EDTA via repeated ultrafiltration (Amicon) and dialysis. For self-cleavage studies the sample was exchanged with 50 mM Tris–HCl, pH 7.5, and 50 mM NaCl by repeated dialysis and ultrafiltration (Amicon). For isothermal titration calorimetry (ITC) experiments the full-length protein was exchanged with 50 mM *N*-(2-hydroxyethyl)piperazine-*N*′-ethanesulfonic acid (HEPES), pH 7.5, and 100 mM NaCl after removing the EDTA by repeated dialysis and ultrafiltration. Fractions with a λ_{max} at 278 nm were pooled and confirmed to be pure human frataxin by sodium dodecyl sulfate (SDS) polyacrylamide gel electrophoresis (PAGE). All apo frataxin samples were stored at –80 °C.

Thrombin removal of His-tag

Full-length human frataxin with an N-terminal His-tag was purified by Ni-NTA affinity chromatography as previously described. The purified protein was subsequently incubated with 100 mM EDTA and 100 μM tris(2-carboxyethyl)phosphine (TCEP) for 4 h. Removal of the His-tag sequence by thrombin-mediated cleavage (GE Healthcare Bio-Sciences, Piscataway, NJ, USA) was performed according to the manufacturer's instructions. Subsequently, the thrombin-digested protein was dialyzed against a buffer containing 40 mM Tris, pH 8.0, 500 mM NaCl and 5 mM imidazole prior to reloading onto the Ni-NTA resin to remove undigested protein and cleaved His-tag. The resin was subsequently washed with five column volumes to recover the His-tag free product. Flow through and wash were combined and concentration was by ultrafiltration (Amicon with an YM10K membrane). This solution was next filtered through a YM30K membrane to remove thrombin and product purity was verified by SDS-PAGE. Buffer exchange of purified His-tag free full-length frataxin was performed on a G-25 desalting column (Aldrich). Concentrations were measured by use of absorbance measurements and the calculated ε at 280 nm (33,260 M^{-1} cm^{-1}).

Metal-promoted cleavage

Metal-promoted cleavage of full-length frataxin was evaluated by SDS-PAGE (20%). Full-length frataxin was isolated using buffer solutions prepared from NANOpure water, as described, exchanged into a reaction buffer (50 mM HEPES, pH 7.5, 100 mM NaCl) by ultrafiltration, and protein concentration was determined from the absorbance at 278 nm. A sample containing 25 μM of full-length frataxin was transferred into several 1.5-mL tubes and 1 mM EDTA was added to remove possible trace metal ions in each aliquot. Finally, 2 mM of various metal ions was added to these tubes to give an effective concentration of each metal of approximately 1 mM. Cleavage reactions were performed at 4 °C for 4 days and stopped by addition of SDS loading buffer. The concentration of truncated frataxin was determined by use of the Bradford assay or absorbance measurements (ε_{280} = 26,030 M^{-1} cm^{-1} for truncated frataxin).

Mass spectrometry

All mass spectra were acquired from the Campus Chemical Instrument Center at Ohio State University. Mass determination was performed by electrospray ionization time-of-flight measurements using a Micromass Q-TOF II (Micromass, Wythenshawe, UK) mass spectrometer equipped with an orthogonal electrospray source (Z-spray) operated in positive ion mode. Background salt was removed from holo frataxin by extensive dialysis against NANOpure water.

ITC quantitation of metal binding and ISU binding to full-length frataxin

ITC measurements of ferrous or manganese ion binding to either His-tagged or thrombin-cleaved full-length apo frataxin were carried out at 25 °C using a MicroCal VP-ITC instrument. The titrant and sample solutions were made up in the same stock buffer solution (50 mM HEPES buffer, pH 7.5, 100 mM NaCl) and both experimental solutions were thoroughly argon-purged and degassed before each titration. For ferrous ion titrations, 2.5 mM dithionite was added to prevent oxidation to the ferric form. The solution in the cell was stirred at 300 rpm by syringe to ensure rapid mixing. Typically, 3–10 μL of titrant (1 mM ferrous iron or manganese in 50 mM HEPES buffer, pH 7.5, 100 mM NaCl) was delivered to a solution of 20–50 μM frataxin over a period of 20 s with an adequate interval (5–10 min) between injections to allow complete equilibration. Titrations continued until 6 equiv had been added to ensure no further complex formation following addition of excess titrant. A control background titration consisting of an identical titrant solution, but containing only the buffer solution in the sample cell, was subtracted from each experimental titration to account for the heat of dilution. SDS-PAGE experiments confirmed that there was no significant cleavage reaction during the ITC measurements.

ITC measurements of human ISU (D37A), a partner protein, binding to either His-tagged or thrombin-cleaved full-length apo frataxin in the presence of a tenfold excess or onefold ferrous iron were carried out at 25 °C. The titrant and sample solutions were made up in the same stock buffer solution (50 mM HEPES buffer, pH 7.5, 100 mM NaCl, 5 mM dithionite), and both experimental solutions were thoroughly argon-purged and degassed before each titration. The solution in the cell was stirred at 300 rpm by syringe to ensure rapid mixing. Typically, 10 μL of titrant (0.4 mM apo human ISU (D37A) in 50 mM HEPES buffer, pH 7.5, 100 mM NaCl) was delivered to a solution of approximately 50 μM frataxin over a period of 20 s with an adequate interval (5–10 min) between injections to allow complete equilibration. Titrations continued until 4 equiv had been added to ensure no

further complex formation following addition of excess titrant. A control background titration consisting of the identical titrant solution, but containing only the buffer solution in the sample cell, was subtracted from each experimental titration to account for the heat of dilution. Again, SDS-PAGE experiments confirmed that there was no significant cleavage reaction during the ITC measurements.

Data were collected automatically and subsequently analyzed with a one-site binding model by the Windows-based Origin software package supplied by MicroCal. The Origin software uses a nonlinear least-squares algorithm (minimization of χ^2) and the concentrations of the titrant and the sample to fit the heat flow per injection to an equilibrium association equation, providing best-fit values of the stoichiometry (n), change in enthalpy (ΔH), change in entropy (ΔS) and binding constant (K_A).

Results

Metal-promoted self-cleavage

Full-length expressed frataxin has an N-terminal His-tag and includes residues 46–210 including the second MPP cleavage site between residues 55 and 56 (Fig. 2a). Thrombin-cleaved protein, lacking the His-tag domain, was also prepared and studied to evaluate the influence of the His-tag sequence on iron binding and cleavage activity. According to SDS-PAGE analysis, the products formed by natural cleavage during purification, and those observed following addition of ferric or ferrous iron to ''full-length'' frataxin, were similar (Figs. 2b, 3), although the efficiency of the iron-promoted cleavage was significantly greater under otherwise similar conditions. Metal-promoted cleavage was also observed following removal of the His-tag residues, and in fact cleavage activity was enhanced.

The cleavage product was further characterized by mass spectrometry. Cavadini et al. [22] had previously reported the mass of the natural cleavage product (degradation) as 14,663 Da, corresponding to the sequence 78–210 of human frataxin, although the origin of the cleavage chemistry was not addressed. Our mass spectrometry analysis of the cleaved product protein in the presence of iron showed a peak with $M_r \sim 14{,}661$, which is consistent with the mass of the natural cleavage product (Fig. 2c). That is, similar results are obtained irrespective of whether one begins with full-length or truncated frataxin in the presence of excess ferrous ion. In addition to the cleavage product, the mass spectrometry results (Fig. 2c) also showed peaks from iron-bound forms of truncated frataxin at 14,775, 14,906 and 15,019 Da, corresponding to two bound irons, four bound irons and six bound irons, respectively, that are consistent with earlier reports of iron binding to truncated human frataxin [9]. Moreover, the mass data are consistent with a binuclear configuration for these irons, similar to the bacterial frataxin orthologue, CyaY [20].

To confirm the involvement of iron (or other metals) in the cleavage reaction, the influence of the metal ion chelator EDTA was determined by monitoring product cleavage by use of SDS-PAGE. Samples containing the same quantity of full-length frataxin were prepared with and without added EDTA (to 1 mM), and with and without iron ion, and maintained at 4 °C for 5 days (Fig. 2b). The cleavage efficiency in the EDTA-treated frataxin sample was severely reduced relative to that in the sample with no added EDTA, in the case of either distilled water or NANOpure water based buffer systems. Furthermore, the amount of cleavage product observed in sample solutions using buffers prepared using distilled water was significantly greater than that in a NANOpure water based buffer system (Fig. 2b), again suggesting a role for trace metal ions in promoting the cleavage reaction.

The selectivity of metal-promoted cleavage was evaluated by SDS-PAGE. Under the usual reaction conditions no cleavage was observed in the presence of Mg^{2+}, Al^{3+}, Ca^{2+}, Co^{2+}, Ni^{2+}, Cu^{2+} or Zn^{2+}, reflecting the absence of catalytic activity and/or poor binding to full-length frataxin. Cleavage was observed in the presence of two first-row divalent transition metals, namely, Fe^{2+} and Mn^{2+} (Fig. 3). Lanes 1 and 2 illustrate the effect of each metal in promoting the cleavage reaction. Promotion of the cleavage reaction had already been demonstrated by ferric ion, consistent with a hydrolytic rather than a redox-promoted cleavage mechanism. However, the ferrous state is physiologically more relevant. The similarity in cleavage activity for Fe^{2+} and Mn^{2+} under aerobic and anaerobic conditions is also consistent with a hydrolytic pathway. In the case of Mn^{2+}, Fenton-type chemistry is precluded by the known aerobic stability of Mn^{2+}(aq).

ITC evaluation of metal ion binding to full-length frataxin

The aforementioned results, combined with data from Figs. 2b and 3, indicate that metal-promoted hydrolysis is the most likely underlying reason for the unexpected N-terminal cleavage of human frataxin in vitro. Accordingly, metal binding to full-length frataxin would be anticipated and was examined by ITC. Divalent manganese was observed to bind with rela-

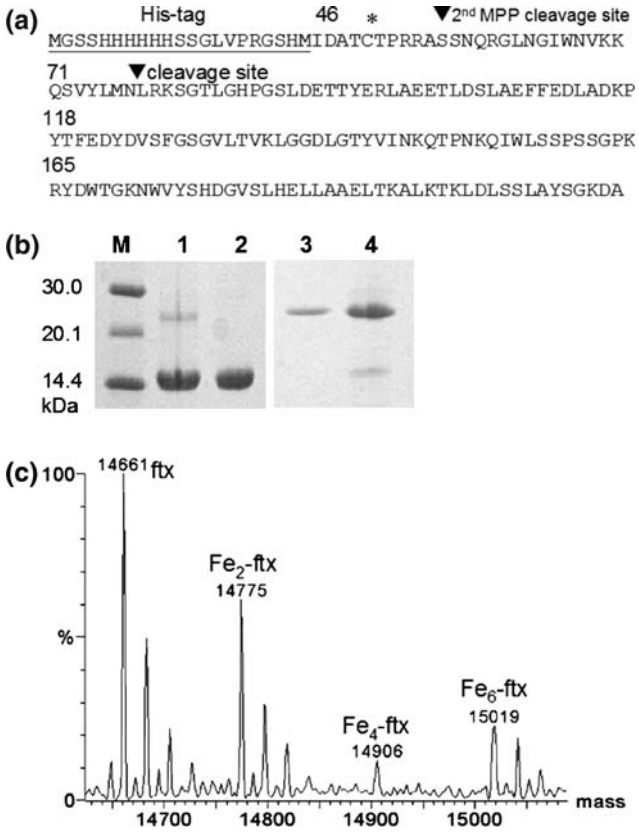

Fig. 2 **a** The gene construct expressing full-length human frataxin carrying an N-terminal His-tag, and showing the second mitochondrial processing peptidase cleavage site and the later self-cleavage site (the iron-mediated cleavage site). Residue Cys50 (*asterisk*) is not present in the truncated protein. **b** *Lanes 1* and *2* show the cleavage product following isolation with no EDTA added to distilled water based buffers (*lane 1*), and the cleavage product following addition of 0.5 mM ferric iron to isolated-full length frataxin (*lane 2*), respectively. Samples were left at 4 °C for 5 days to allow the reaction to develop and the products from both cleavage reactions have essentially the same mass as defined by sodium dodecyl sulfate polyacrylamide gel electrophoresis. *Lanes 3* and *4* show products from sample aliquots in NANOpure water based buffers that were maintained at 4 °C for 5 days with (*lane 3*) or without added EDTA (to 1 mM) (*lane 4*), respectively, with no addition of iron to either. The lower band intensity in *lane 3* reflects loading variances. *Lane M* represents the molecular weight markers. **c** Electrospray ionization mass spectrometry data for holo frataxin showing the mass of the ferrous ion meditated cleavage product as 14,661 Da. Peaks at 14,775, 14,906 and 15,019 Da correspond to two-, four- and six-iron-bound forms of truncated human frataxin. *MPP* mitochondrial processing peptidase, *ftx* frataxin

tively low affinity ($n \sim 1.0$, $K_D \sim 10.3$ μM; Fig. 4, right), compared with binding of ferrous iron ($n \sim 1.0$, $K_D \sim 0.3$ μM; Fig. 4, left). Interestingly, we were unable to observe additional ferrous iron-binding sites in this full-length human frataxin, in marked contrast to the iron-binding properties of the truncated human frataxin, which demonstrated approximately more weakly bound ions ($K_D \sim 55$ μM) [9]. Thrombin-

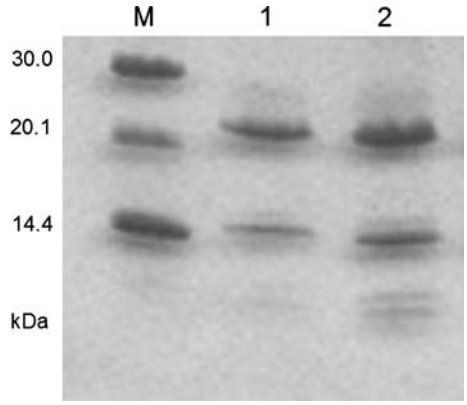

Fig. 3 Comparison of Mn^{2+} (*lane 1*) and Fe^{2+} (*lane 2*) cleavage reactions. Iron was maintained in the ferrous state by addition of 5 mM dithionite, while all procedures were performed under argon in a glove bag. Reactions were maintained at 4 °C for 4 days

cleaved full-length human frataxin, lacking the His-tag sequence, also retained the unique iron-binding site ($n \sim 1.0$, $K_D \sim 4$ μM), with the His-tag conveying a slight stabilization of the bound iron.

Impact of the N-terminal domain on frataxin binding to ISU

It was earlier stated that a predicted consequence of binding of the N-terminal domain of full-length frataxin to the carboxylate-rich surface around the α1-helix and the β1-sheet would be inhibition of iron binding to the previously characterized lower-affinity binding sites [9] and an inhibitory effect on the binding of partner proteins such as the Fe–S cluster scaffold protein ISU. In fact, other than the unique high-affinity site, no significant iron binding is exhibited by full-length frataxin. Moreover, Fig. 5 shows that the affinity of full-length frataxin for human ISU is diminished almost 40-fold relative to the truncated form ($K_D \sim 0.15$ μM for truncated [9] and $K_D \sim 5.4$ μM for the full-length form), and occurs only in the presence of a large excess of ferrous ion that facilitates competitive displacement of the N-terminal domain of full-length frataxin. Similar to the truncated protein, no binding of full-length frataxin to ISU was detected in the absence of an excess of iron ions, which presumably populate the lower-affinity sites on the anionic surface (Fig. 1) and promote cross-linking of the two proteins, as previously suggested [9]. While we had earlier noted that the lower-affinity sites were not readily populated by iron ion for the full-length frataxin, the presence of a binding partner creates a coordination environment in the protein–protein complex that enhances the binding affinity for at least some of these sites, and

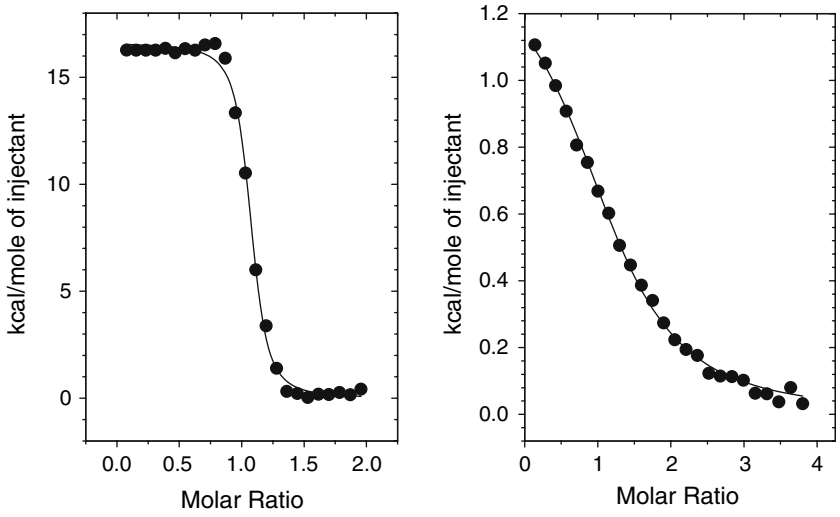

Fig. 4 Isothermal titration calorimetry of full-length human frataxin titrated with (*left*) ferrous iron ($n \sim 1.0$, $K_D \sim 0.3$ μM) and (*right*) manganese ($n \sim 1.0$, $K_D \sim 10.3$ μM). For the ferrous iron titration, 2.5 mM dithionite was also added to maintain the ferrous state. Experimental details are provided in "Materials and methods"

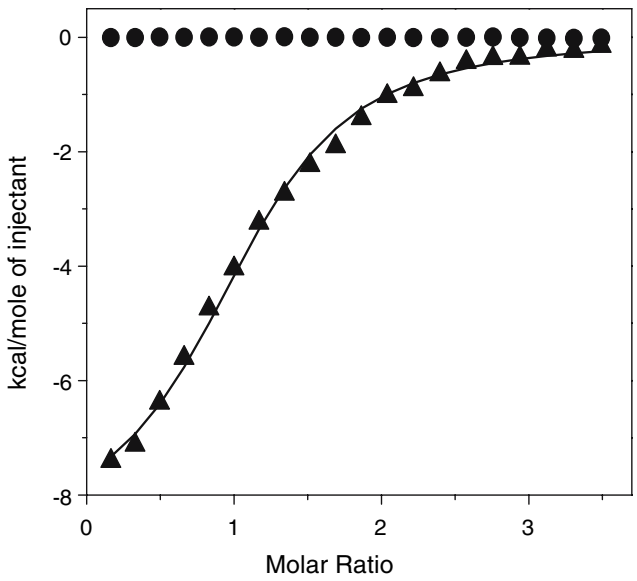

Fig. 5 Isothermal titration calorimetry of full-length human frataxin titrated with human ISU (D37A) in the presence of various amounts of ferrous ion. The *triangles* correspond to ISU binding to frataxin in the presence of a tenfold excess of ferrous ion (stoichiometry $n \sim 1.1$, $K_D \sim 5.4$ μM), while the *circles* correspond to ISU titration of frataxin in the presence of a 1:1 ratio of ferrous ion to frataxin (with no evidence of binding). Both experiments also included 5 mM dithionite to maintain the oxidation state of iron as ferrous. Experimental details are provided in "Materials and methods"

provides for modest binding of ISU to full-length frataxin in the presence of excess iron.

Discussion

Posttranslational modification by autoproteolysis is a mechanism whereby proteins may activate themselves and/or incorporate multiple functions within a single polypeptide chain [23–25]. Ovotransferrin falls into this category, undergoing redox-dependent autoproteolysis [23]. Many groups have observed the unexpected N-terminal cleavage of human frataxin in vitro [9, 17, 18], although the underlying chemistry and significance have been ignored. We also observed the same pattern of cleavage during purification, but noted the cleavage activity to be particularly prominent following treatment with iron ion (Fig. 2b). Both SDS-PAGE and mass spectrometry data suggested a role for iron in promoting the cleavage reaction. Aside from any potential physiological relevance, the self-cleavage is clearly of intrinsic and practical interest.

ITC experiments clearly demonstrated the multiple low-affinity iron-binding sites observed for truncated human frataxin to be blocked in the case of the full-length protein (Fig. 4), which displayed a distinct high-affinity iron-binding site that promoted catalytic cleavage and resulted in formation of the truncated form. Such a cleavage product has been reported not only in recombinant human frataxin, but was also identified in human heart extract [26]. In spite of the observed activity of Mn(II) in promoting cleavage, iron is clearly the physiologically relevant metal, given the relatively high concentration of bioavailable iron ion in the mitochondrion (up to 10 μM) [27]. It is likely that this iron-promoted cleavage reaction is relevant to cellular chemistry, since full-length human frataxin shows a significantly lower (and nonphysiological) affinity for the Fe–S cluster scaffold protein ISU [9] (Fig. 5), or ferrochelatase [10], either in the presence or in the absence of ferrous ion.

We earlier hypothesized that the N-terminal domain of full-length frataxin stabilizes a higher-affinity iron-

binding site and that charged residues in the N-terminal domain make electrostatic contacts with the carboxylate-rich surface around the α1-helix and the β1-sheet, blocking further binding to the weaker iron-binding sites and inhibiting binding of partner proteins. It appears that the N-terminal domain is readily released from the anionic surface following iron-promoted cleavage. This conclusion is consistent with observations from ITC experiments that show full-length human frataxin to bind a unique high-affinity iron, while truncated human frataxin has multiple, relatively low affinity iron-binding sites. Recently, Nair et al. [20] proposed specific iron-binding sites of truncated human frataxin by solution NMR experiments. As previously predicted [9], the binding sites were located in the negatively charged anionic surface around the α1-helix and the β1-sheet. They also reported that iron-binding sites of human frataxin were similar to those of the bacterial frataxin orthologue, CyaY. Moreover, these data are also consistent with that reported by He et al. [21] for the yeast frataxin homologue.

Our results show that iron ion both binds to a unique high-affinity site and promotes hydrolytic cleavage of the N-terminal domain in MPP-processed protein that makes available a distinct set of lower-affinity iron-binding sites. While the full-length protein shows a unique iron-binding site with $K_D \sim 0.3$ μM, the truncated human frataxin displays multiple iron-binding sites with $K_D \sim 10.3$ μM for ferric ion and $K_D \sim 55$ μM for ferrous ion [9]. Presumably the metal at the higher-affinity site functions as a Lewis acid catalyst that provides transition-state stabilization during hydrolysis. While the presence of the His-tag sequence modestly stabilizes the unique iron site in full-length frataxin, the affinity remains submicromolar following removal of the His-tag sequence. Moreover, the rate of metal-promoted cleavage is significantly enhanced; most likely reflecting improved steric access to the cleavage site.

A plausible structural mechanism for blocking of the anionic surface by N-terminal residues in full-length frataxin, preventing iron binding to the negatively charged surface (Fig. 1), would be through multiple electrostatic contacts involving some of the many positively charged residues in the N-terminus of frataxin, including Arg60, Lys69, Lys70, Arg79 and Lys80, and carboxylates on the anionic surface (Fig. 1). Both crystallographic data [19] and solution NMR structures [18] suggest the structural core of frataxin (residues 88–210) to be rigid; however, Musco et al. [18] have reported that the N-terminal residues (75–90) might be unfolded on the basis of circular dichroism and NMR spectroscopy results, but were unable to directly observe the structure as a result of cleavage. Interestingly, He et al. [21] recently reported the overall structure of the yeast frataxin homologue and found the N-terminus, which has a 310-helix, to lie toward the α1-helix and the β1-sheet of the core structure. This result is, of course, consistent with the results of the studies reported herein, where the N-terminal domain is envisaged to lie across and block access to the anionic surface shown in Fig. 1. To be functionally active as an iron-delivery vehicle to target proteins, this interaction should be eliminated by removal of the N-terminus.

O'Neill et al. [26] recently reported that supramolecular assemblies of full-length human frataxin are stabilized by subunit–subunit interactions of the N-terminal residues. It has also been suggested that such self-assembly reactions of frataxin provide a detoxification mechanism for redox-active iron [28]. However, Aloria et al. [29] have reported that oligomerization of yeast frataxin (Yfh1) and oligomerization-induced iron storage are not critical cellular functions of frataxin. In our hands the formation of multimeric complexes of full-length human frataxin was never observed for the iron-bound form, and only inconsistently for the apo form as judged by gel filtration experiments. Such variations in aggregation state and mineral formation may reflect variations in experimental conditions and the cell source of frataxin; however, the significance for cellular function remains uncertain.

Published data support a role for frataxin in mediating delivery of iron to target proteins, including ISU, ferrochelatase and aconitase [9–12, 14–16]. Moreover, several groups [9, 20, 21, 30] have suggested that multiple iron ions bind to the anionic surface of frataxin (Fig. 1). The results described herein support a simple functional model for the structural chemistry of the N-terminal domain of full-length human frataxin and its potential role to control the masking or opening of the anionic α1/β1surface (possibly synchronizing iron influx into the matrix with delivery to target proteins). Iron binding to the high-affinity site of full-length frataxin weakens the interaction of the N-terminal domain with the acidic α1/β1 surface and promotes cleavage of the N-terminus to openly reveal the acidic surface that can then freely interact with partner proteins and mediate iron delivery. Alternatively, if cellular cleavage were relatively slow, the iron-bound full-length protein might interact with specific partners, but with reduced binding affinity. Such a mechanism would prevent nonspecific interactions with other protein partners or charged species in the absence of a critical concentration of iron.

Overall, the results described herein suggest a structural gating role for the N-terminal residues of

human frataxin and suggest a complex cellular function in the regulation and delivery of cellular iron. Inasmuch as prior solution studies on human frataxin have focused on the truncated version, the results presented here help to bridge the gap between the characterized chemistry of truncated frataxin with physiological partners and the full-length protein produced by cellular proteolytic processing. In fact, the absence of significant binding to physiological partners in the full-length form suggests that further processing may occur within the cell to form the activated truncated version.

Acknowledgements This work was supported by a grant the National Science Foundation, CHE-0111161.

References

1. Babcock M, de Silva D, Oaks R, Davis-Kaplan S, Jiralerspong S, Montermini L, Pandolfo M, Kaplan J (1997) Science 276:1709–1712
2. Cavadini P, Gellera C, Patel PI, Isaya G (2000) Hum Mol Genet 9:2523–2530
3. Puccio H, Simon D, Cossee M, Criqui-Filipe P, Tiziano F, Melki J, Hindelang C, Matyas R, Rustin P, Koenig M (2001) Nat Genet 27:181–186
4. Foury F, Cazzalini O (1997) FEBS Lett 411:373–377
5. Koutnikova H, Campuzano V, Foury F, Dolle P, Cazzalini O, Koenig M (1997) Nat Genet 16:345–351
6. Campuzano V, Montermini L, Molto MD, Pianese L, Cossee M, Cavalcanti F, Monros E, Rodius F, Duclos F, Monticelli A, Zara F, Canizares J, Koutnikova H, Bidichandani SI, Gellera C, Brice A, Trouillas P, De Michele G, Filla A, De Frutos R, Palau F, Patel PI, Di Donato S, Mandel JL, Cocozza S, Koenig M, Pandolfo M (1996) Science 271:1423–1427
7. Patel P, Isaya G (2001) Am J Hum Genet 69:15–24
8. Wong A, Yang J, Cavadini P, Gellera C, Lonnerdal B, Taroni F, Cortopassi G (1999) Hum Mol Genet 8:425–430
9. Yoon T, Cowan JA (2003) J Am Chem Soc 125:6078–6084
10. Yoon T, Cowan JA (2004) J Biol Chem 279:25943–25946
11. Bulteau AL, O'Neill HA, Kennedy MC, Ikeda-Saito M, Isaya G, Szweda LI (2004) Science 305:242–245
12. Park S, Gakh O, O'Neill HA, Mangravita A, Nichol H, Ferreira GC, Isaya G (2003) J Biol Chem 278:31340–31351
13. Muhlenhoff U, Richhardt N, Ristow M, Kispal G, Lill R (2002) Hum Mol Genet 11:2025–2036
14. Gerber J, Muhlenhoff U, Lill R (2003) EMBO Rep 4:906–911
15. Lesuisse E, Santos R, Matzanke BF, Knight SA, Camadro JM, Dancis A (2003) Hum Mol Genet 12:879–889
16. Ramazzotti A, Vanmansart V, Foury F (2004) FEBS Lett 557:215–220
17. Cavadini P, Adamec J, Taroni F, Gakh O, Isaya G (2000) J Biol Chem 275:41469–41475
18. Musco G, Stier G, Kolmerer B, Adinolfi S, Martin S, Frenkiel T, Gibson T, Pastore A (2000) Structure 8:695–707
19. Dhe-Paganon S, Shigeta R, Chi Y, Ristow M, Shoelson SE (2000) J Biol Chem 275:30753–30756
20. Nair M, Adinolfi S, Pastore C, Kelly G, Temussi P, Pastore A (2004) Structure 12:2037–2048
21. He Y, Alam S, Proteasa S, Zhang Y, Lesuisse E, Dancis A, Stemmler T (2004) Biochemistry 43:16254–16262
22. Cavadini P, O'Neill HA, Benada O, Isaya G (2002) Hum Mol Genet 11:217–227
23. Ibrahim HR, Haraguchi T, Aoki T (2006) Biochim Biophys Acta 1760:347–355
24. Jeffery CJ (2003) Trends Genet 19:415–417
25. Perler FB (1997) Curr Opin Chem Biol 1997:292–299
26. O'Neill H, Gakh O, Isaya G (2005) J Mol Biol 345:433–439
27. Petrat F, de Groot H, Rauen U (2001) Biochem J 356:61–69
28. O'Neill H, Gakh O, Park S, Cui J, Mooney S, Sampson M, Ferreira G, Isaya G (2005) Biochemistry 44:537–545
29. Aloria K, Schilke B, Andrew A, Craig EA (2004) EMBO Rep 5:1096–1101
30. Bou-Abdallah F, Adinolfi S, Pastore A, Laue TM, Chasteen ND (2004) J Mol Biol 341:605–615